THE ASTROPHYSICAL JOURNAL, **187**:369–375, 1974 January 15

THE SPATIAL DISTRIBUTION OF LYMAN-α ON THE SUN

D. K. PRINZ
E. O. Hulburt Center for Space Research, Naval Research Laboratory, Washington, D.C.
Received 1973 June 25; revised 1973 August 24

ABSTRACT

One of the high spatial resolution, Lα line spectroheliograms obtained by the Naval Research Laboratory during a rocket flight on 1972 July 10 has been analyzed to show the distribution of Lα on the solar disk. The intensity distribution across selected cells, filaments, bright "points," and active regions is presented. The distribution of intensity with respect to area on the projected disk is shown to have a peak at $\sim 3.8 \times 10^{15}$ photons cm^{-2} s^{-1} sterad^{-1}. Setting an upper limit to the intensity from cells, the north-south distribution of the integrated flux from cells is shown to be within 20 percent of that expected from a sphere having a uniform intensity except in the regions where active areas are prominent. The total flux at the Earth, 3.25×10^{11} photons cm^{-2} s^{-1}, agrees well with the Lα flux measured the previous day by the French OSO-5 experiment. It is reasoned that the variability of the total Lα flux may be due not only to the variations in the plage areas, but also to variations in the average cell intensity.
Subject headings: solar activity — spectroheliograms — ultraviolet

I. INTRODUCTION

In a previous paper (Prinz 1973) preliminary results from the high spatial resolution Lα spectroheliograms obtained by the U.S. Naval Research Laboratory during a rocket flight on 1972 July 10 were presented. Further analysis of those data is given herein. We show (1) the intensity distribution for some specific features, (2) the distribution of intensity with respect to area on the flat disk, and (3) the north-south distribution of both the total flux and the flux from cells alone.

In this paper we use the term "intensity" to denote the number of Lα photons emitted in 1 second by 1 square centimeter of the flat (projected) Sun into a solid angle of 1 steradian in a direction parallel to the pointing axis of the instrument. Other authors have called this quantity "brightness" (Gabriel 1971), "radiance" (Pivovonsky and Nagel 1961), or "photon sterance" (Nicodemus 1972). We chose intensity because that is the terminology commonly used in radiative transfer theory (Chandrasekhar 1960), albeit our "photons" should be converted to units of energy for exact correspondence.

II. THE DISTRIBUTION OF INTENSITY FOR SPECIFIC FEATURES

Figure 1 (plate 4) is an enlargement of one of the solar Lα images taken at 21:07 hours (UT). The arrows indicate the position and direction of microdensitometer scans over specific features; the beginning of the tail of the arrow marks the start of the scan, the tip of the arrow the end. The numeral to which each arrow points is the label for that scan.

The square densitometer slit corresponded to an angular region approximately $3'' \times 3''$; the density was recorded at $0''.2$ intervals and converted to flux at the Earth as described previously (Prinz 1973). To convert the incident flux to solar intensity, we divided by the solid angle subtended at the Earth by the area on the projected flat Sun corresponding to the area of the densitometer slit.

Figures 2, 3, and 4 show the intensity distribution through the features labeled 1–13 in figure 1. Figure 2 shows the distribution through four cells (labeled 1–4 in fig. 1). Figure 3 shows the distribution through three small, more-or-less isolated bright regions which we call "points" (labeled 5–7) and through two filaments (labeled 8–10). For the filament near the equator we show two scans (labeled 8 and 9), one in a westerly direction (8) and one in a northerly direction (9). Figure 4 shows the distribution through two active areas. Scans 11 and 12 are in the vicinity of the largest single sunspot present on that day (McMath No. 11947) while scan 13 is in the vicinity of the largest sunspot group (No. 11949). The Ca K plage areas reported for the two sunspot regions were, in millionths of the solar hemisphere, 2800, and 3500, respectively.

The uncertainty in the ordinate in figures 2–4 is ± 20 percent for intensities above about 2×10^{15} photons cm^{-2} s^{-1} sterad^{-1}. Below that value, which approximately corresponds to the onset of the toe of the H-D curve, the uncertainty increases.

The features scanned in figure 1 were chosen to illustrate the following comments:

1) The average width of the cells, i.e., the distance between the peak intensity on opposite sides of the cell, is $\sim(3 \pm 1.5) \times 10^4$ km or $\sim 40'' \pm 20''$. The average width of the boundaries at half the maximum intensity is $\sim 1.5 \times 10^4$ km or $20''$, if secondary peaks are not present. The cell boundaries and active regions typically have $2''$–$10''$ structure, which may be

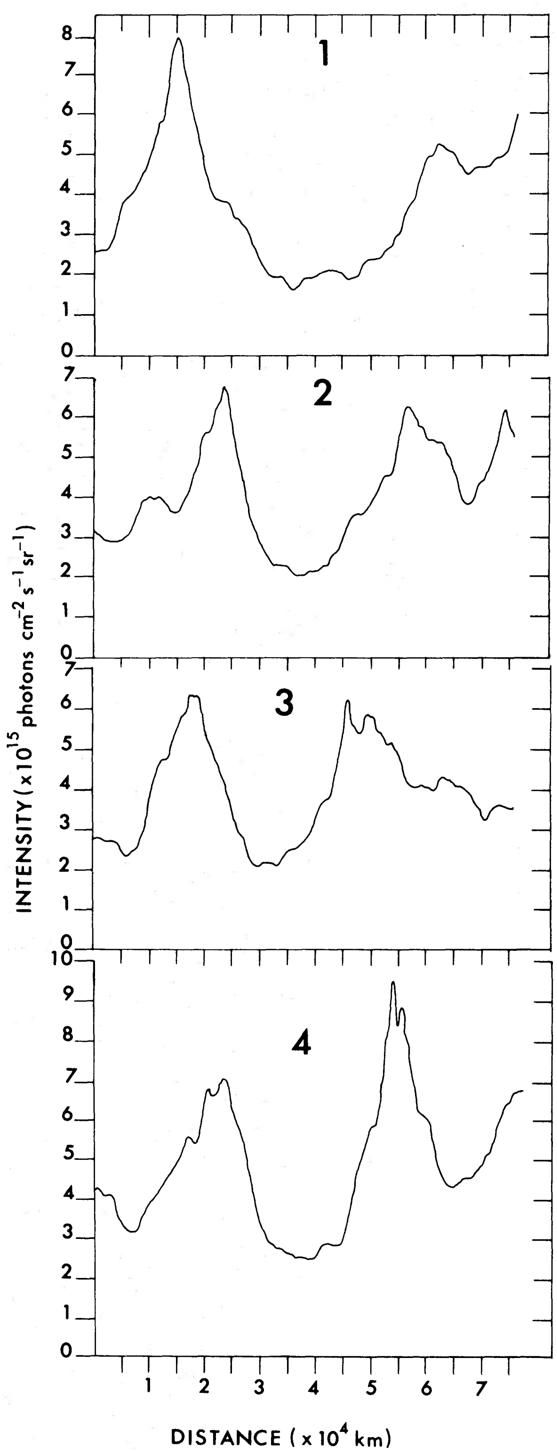

FIG. 2.—The intensity distribution across four of the larger cells. The numbers 1, 2, 3, and 4 correspond to the labeling in fig. 1. Each side of the square densitometer slit used to obtain figs. 2–4 corresponded to a distance of $\sim 2.3 \times 10^3$ km on the projected disk. The density was recorded at intervals corresponding to ~ 150 km.

the manifestation of the tops of spicules or spicule clusters.

2) The more-or-less isolated bright points have peak intensities corresponding to the peak intensities of the cell boundaries, suggesting that they are the remnants thereof.

3) The emission from the center of the cells is of the same order of magnitude as the emission from the dark filaments, although it is within the filaments that the regions of least emission are found.

4) As expected from spectroheliograms in other emission ultraviolet lines, the intensity is high in the vicinity of sunspots.

III. THE DISTRIBUTION OF INTENSITY OVER THE DISK

A raster-microdensitometer scan was made over the entire image shown enlarged in figure 1. The rastering interval, vertically and horizontally, corresponded to $\sim 2''$ steps on the flat disk. This interval, which is 10 times larger than that used to obtain figures 2–4, was necessitated by the computer program available at that time. The density was recorded on magnetic tape. A computer then counted the number of points having density values between two previously set limits. By selecting the density limits so as to correspond to selected intensity intervals using the H-D curve for the film, the histogram in figure 5 was constructed. The total number of points having densities above the background was equated to the total flat disk area. The size of the rastering interval and the $3'' \times 3''$ densitometer slit size have to some extent averaged out the extremas of the intensity. The largest uncertainty in the percent area occurs for intensities below about 2×10^{15} photons cm^{-2} s^{-1} sterad^{-1}, both because of the toe of the H-D curve and because of the upper limit set for the background density.

The peak of the histograms occurs at an intensity interval corresponding approximately to half the maximum intensity from the cell boundaries. The cells (and filaments) are the prime contributors to the intensity below about 7.7×10^{15} cm^{-2} s^{-1} sterad^{-1}; the active regions are the prime contributors above. If we set 7.7×10^{15} photons cm^{-2} s^{-1} sterad^{-1} as the upper limit characteristic of cells, about 73 percent of the total intensity on 1972 July 10 came from cells (and filaments) which covered about 88 percent of the total flat-disk area. The remaining 27 percent of the total intensity came from active areas covering ~ 12 percent of the flat disk.

No correction was made for the overlapped image which comprises the data over about 17 percent of the disk. The intensity interval corresponding to the peak is probably shifted toward a higher value and may be larger with respect to area than it should be. Thus, the relative values given above for the cell versus active regions should be considered preliminary and only approximate.

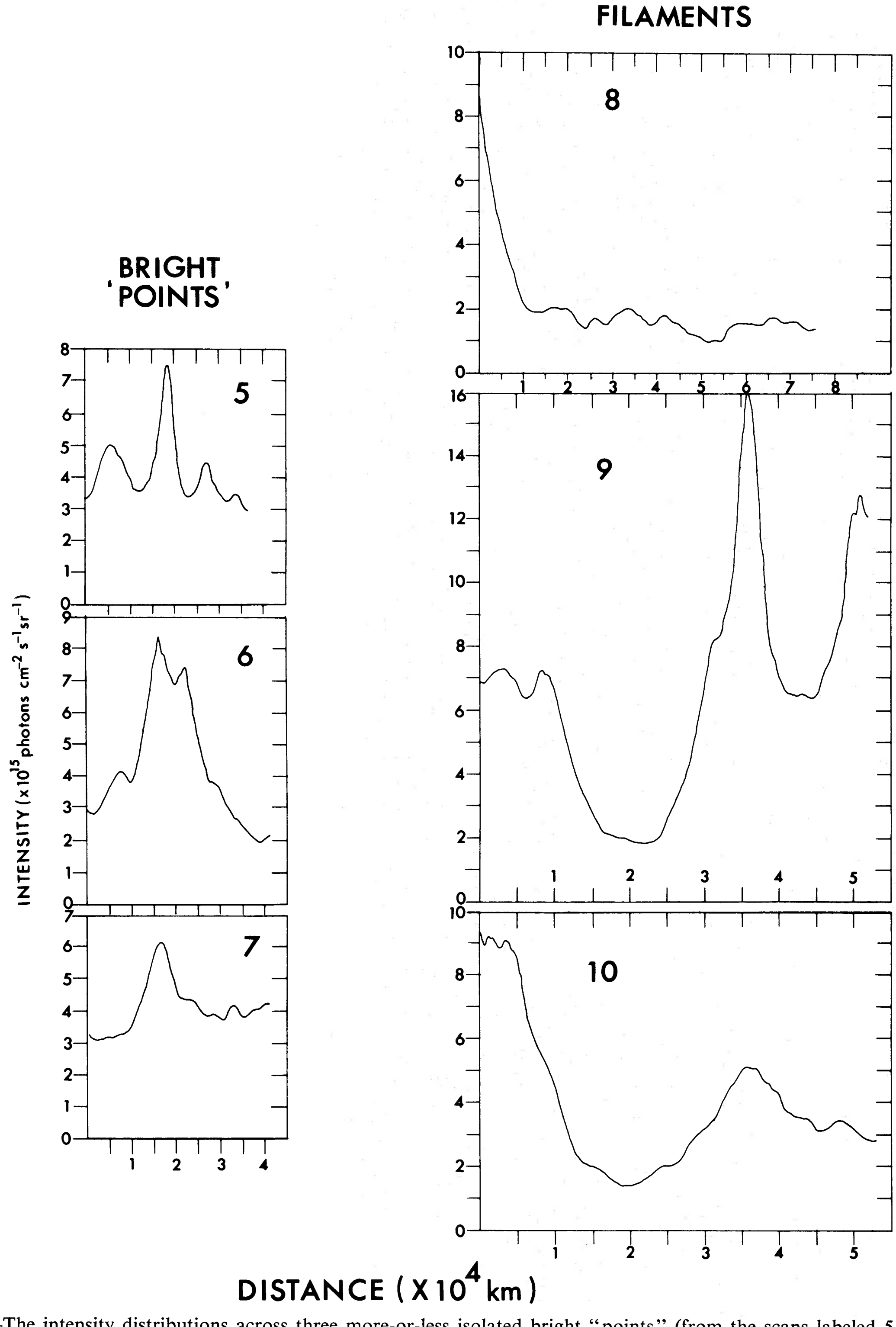

FIG. 3.—The intensity distributions across three more-or-less isolated bright "points" (from the scans labeled 5, 6, and 7 in fig. 1) are shown on the left side of the figure. Scans 8 and 9 show the intensity along and across a filament; scan 10 shows the intensity across a second filament.

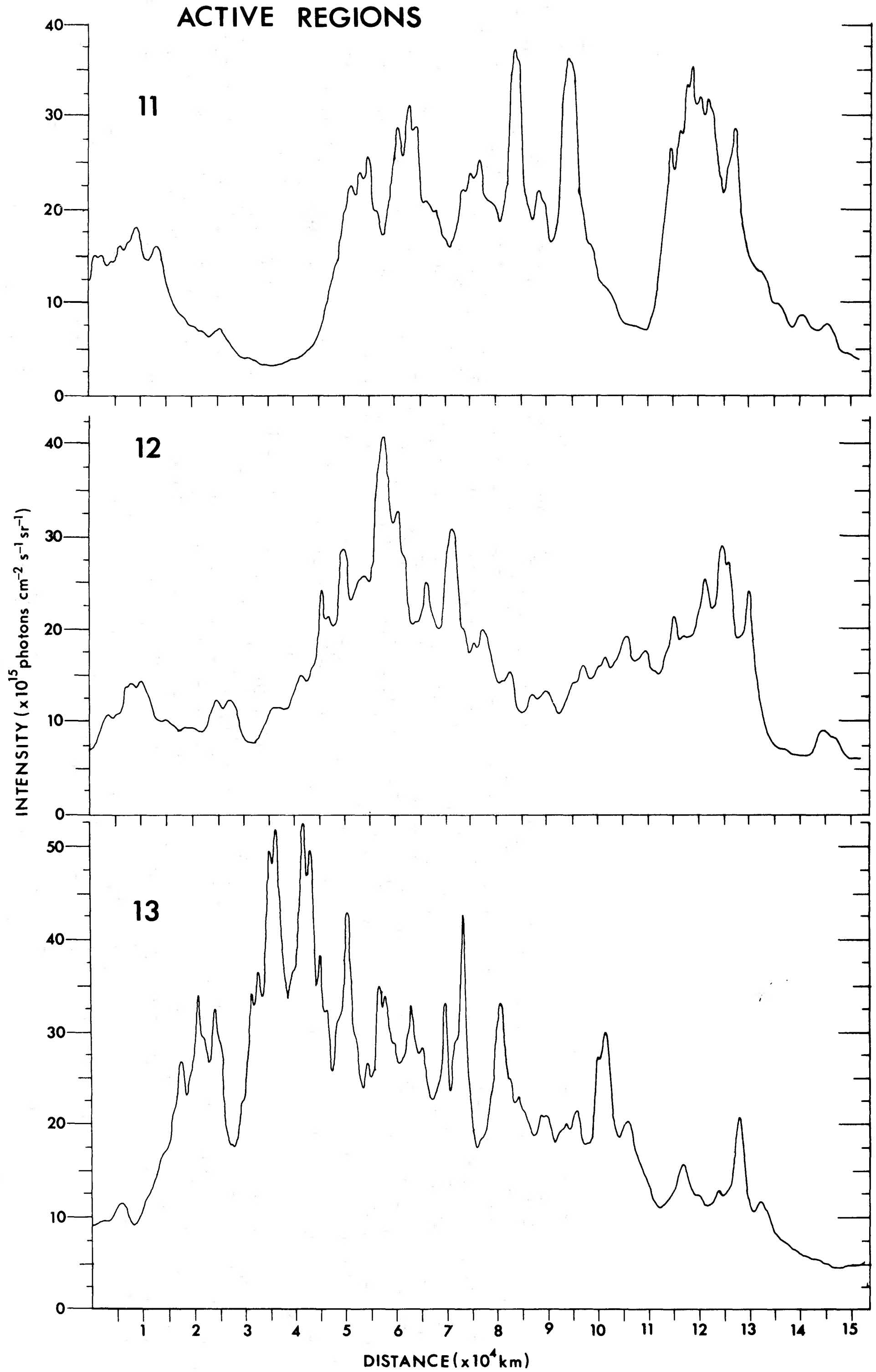

FIG. 4.—The intensity distribution across active regions in the vicinity of two sunspot groups. Scans 11 and 12 are in the vicinity of the largest single sunspot present on the day of the flight. Scan 13 is in the vicinity of a sunspot group having the largest Ca K plage area.

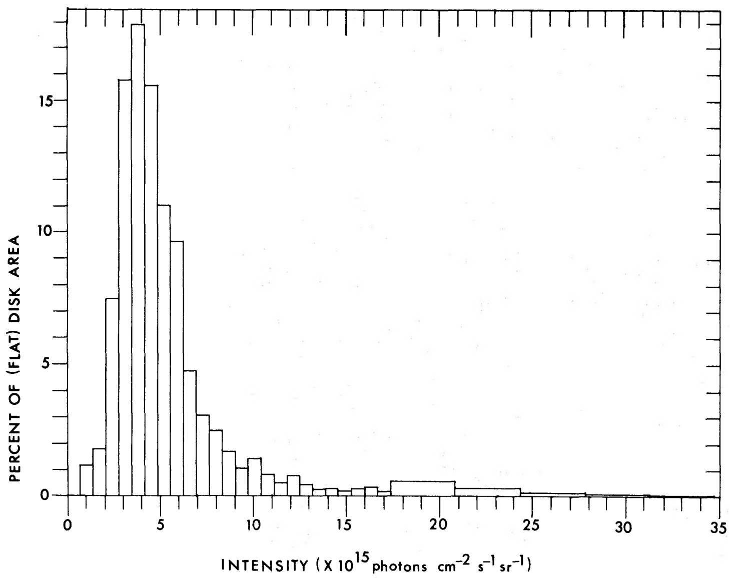

FIG. 5.—A histogram showing the percentage of the projected disk area emitting Lα within successive intensity intervals

Figure 6 is another presentation of the data obtained in the raster scan. We summed the flux from successive sets of 10 lines, which corresponds to $\sim 20''.6$ intervals along the north-south axis, to obtain the total flux within that section of the disk. We arbitrarily set the previously mentioned 7.7×10^{15} photons cm^{-2} s^{-1} sterad^{-1} intensity value as the upper limit characteristic of cells and summed the flux for 10 lines, accumulating only those points having intensities less than this value, calling this the flux from cells.

Values of the flux in the southern hemisphere have been approximately corrected for the overlapping image in the following way: (To simplify the discussion, let A be a symbolic representation of regions where the Lα image alone is present; let O represent regions in the narrow crescent where the overlapping image alone is present; let B represent regions containing both Lα and the overlapping image.) The intensity in each $20''.6$ section comes mainly from an A part and a B part. Since the overlapping occurs principally in regions of cell structure and since each section contains many cells, it was assumed that the average intensity in the A and B parts would have been approximately the same, if the overlapping image had not been present. To correct for the enhanced intensity in B, we estimated the fraction, f, of the area in each section containing B. By scanning regions in O and adjacent regions of similar structure in B, an average ratio, g, of intensity of the two (O/B) was calculated. The measured intensity was then multiplied by the fraction $[1 + f(g/(1 - g))]^{-1}$.

From figure 6, it can be seen that as active regions become dominant, the flux from cells is depleted. With the exception of the depleted areas, the flux from the cells is similar to what would be expected from a flat disk (or sphere) of uniform intensity when summed in the same manner as the solar image. To compare the cell flux with that from a uniform disk two parameters must be chosen: the intensity of the disk and the diameter. For the intensity we chose 3.8×10^{15} photons cm^{-2} s^{-1} sterad^{-1}, which corresponds to the peak of the histogram in figure 5. Although the exact angular diameter of the Lα image is difficult to define, both because of the structure at the limb and because of the uncertainty in the angular calibration of the instrument, we determined it to be between $31'.3$ and $31'.8$. The apparent visible angular diameter was $31'.513$ (from the *American Ephemeris and Nautical Almanac*). We chose $31'.6$ as an approximate angular diameter for the uniform disk. The resultant flux is given by the dashed curve in figure 6. For the northernmost $2'$ the measured flux is lessened by the notch created in the Lα image by mispointing of the instrument (see Prinz 1973). The chosen parameters for the uniform disk are observed to be a compromise fit between the measured flux for the polar and equatorial regions, the difference being <20 percent except in strong active regions. Also, there is no significant limb brightening or darkening.

IV. THE TOTAL Lα FLUX

By adding the intensities obtained in the raster scan, we obtained a total Lα flux at the Earth on 1972 July 10 of 3.25×10^{11} photons cm^{-2} s^{-1}. This number has been corrected for the absorption by residual water vapor present in the payload (see Prinz 1973) and approximately corrected for the contribution due to the overlapped portion of the image. The uncertainty in the total flux is about ± 20 percent. From that part

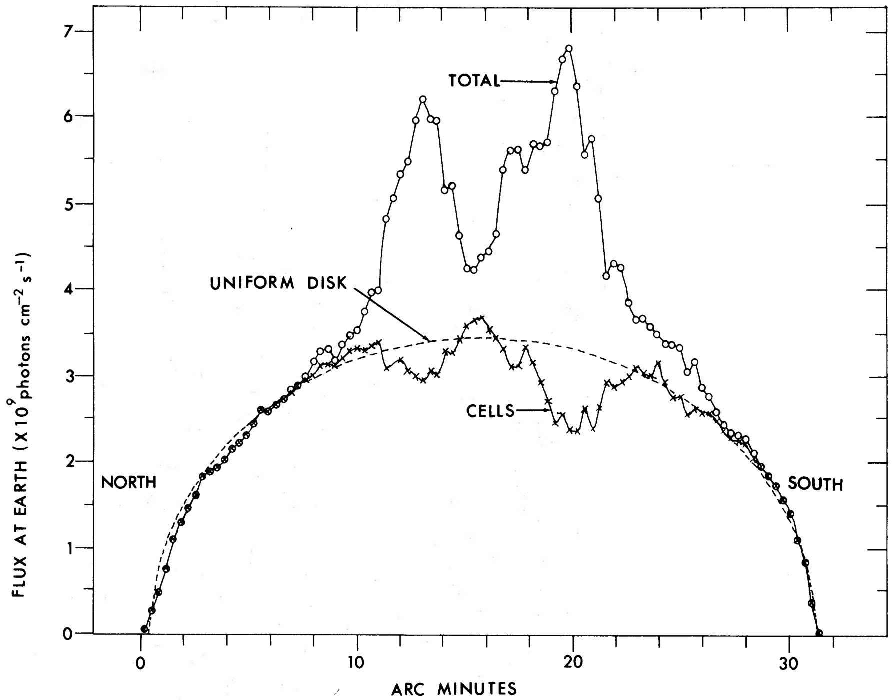

FIG. 6.—The flux at the Earth from sections of the projected disk summed over $\sim 20''.6$ intervals along the north-south axis. The circles show the values for the total flux from the sections; the crosses are the flux values from regions within each section having an intensity less than 7.7×10^{15} photons $cm^{-2}\ s^{-1}$ $sterad^{-1}$, which is arbitrarily set as the upper limit of the cells' intensity. The circles and crosses are connected by a smooth curve for visual clarity. The dashed curve connects valves for a uniform sphere of intensity 3.8×10^{15} photons $cm^{-2}\ s^{-1}$ $sterad^{-1}$, summed in the same manner as the solar image.

of the French OSO-5 Lα experiment which measured the total solar flux in the 100 Å bandpass centered at Lα, J. Blamont and A. Vidal-Madjar (private communications) obtained 3.02×10^{11} photons $cm^{-2}\ s^{-1}$ on 1972 July 9. The flux during the month of July varied about 11 percent. Blamont gives the uncertainty in his value of the flux as perhaps as large as ± 13 percent due to uncertainty in the correction for aging of the detector. The 8 percent difference between the French and NRL measurements is easily covered by the uncertainty in either measurement. The average of the French OSO-5 and the NRL measurements for the total flux on 1972 July 10 is then 3.14×10^{11} photons $cm^{-2}\ s^{-1}$, with a lower limiting value based on the uncertainties of 2.6×10^{11} photons $cm^{-2}\ s^{-1}$.

V. VARIABILITY OF THE COMPOSITION OF THE TOTAL FLUX

We now consider the question of whether the variations observed in the total Lα flux could be due to variations in the flux from active areas alone. That is, we consider the possibility that as active areas decay they are replaced by cells, the average intensity from cells remaining constant so that the total flux from the cells along is increased solely by the increasing area they occupy on the disk. In support of an affirmative answer to the posed question is the approximate correlation between the total Lα flux and the Zurich sunspot number given by Vidal-Madjar, Blamont, and Phissamay (1973) and our observation of increased Lα emission in the vicinity of sunspots.

If we hypothetically replace the active areas with cells on 1972 July 10 we predict the total flux from a completely quiet Sun to be 2.6×10^{11} photons $cm^{-2}\ s^{-1}$ (using the average value of the OSO-5 and NRL measurements), with a lower limiting value of 2.16×10^{11} photons $cm^{-2}\ s^{-1}$. The lowest reported flux measurements by Vidal-Madjar *et al.* (1973) during the 2-year period 1969–1970 was indeed 2.16×10^{11} photons $cm^{-2}\ s^{-1}$ on the 221.22 day of 1970. However, the Zurich sunspot number was in the low 70's and the Ca K spectroheliograms for that day show that some active areas were present. For other periods in 1970 when the sunspot number was lower, 50–60, but plages were still present in the Ca K spectroheliograms, Vidal-Madjar *et al.* observed flux values between 2.3–2.6×10^{11} photons $cm^{-2}\ s^{-1}$. Since these low flux measurements fall within our predicted values for a completely quiet Sun when the Sun was, in fact, not completely quiet, the implication seems to be that the average intensity of the cells is not constant. However, since the contribution to the total intensity from active areas is not known for the

OSO-5 measurements, a definite conclusion awaits future observations.

Useful discussions with Dr. G. E. Brueckner, K. Nicolas, and M. E. Van Hoosier and helpful suggestions by the referee are gratefully acknowledged. J. E. Blamont and A. Vidal-Madjar are thanked for graciously providing their unpublished OSO-5 results.

REFERENCES

Chandrasekhar, S. 1960, *Radiative Transfer* (New York: Dover).
Gabriel, A. H. 1971, *Solar Phys.*, **21**, 392.
Nicodemus, Fred E. 1972, *Opt. Eng.*, **11**, G14.
Pivovonsky, Mark, and Nagel, Max R. 1961, *Tables of Black-body Radiation Functions* (New York: Macmillan).
Prinz, D. K. 1973, *Solar Phys.*, **28**, 35.
Vidal-Madjar, A., Blamont, J. E., and Phissamay, B. 1973, *J. Geophys. Res.*, **78**, 1115.

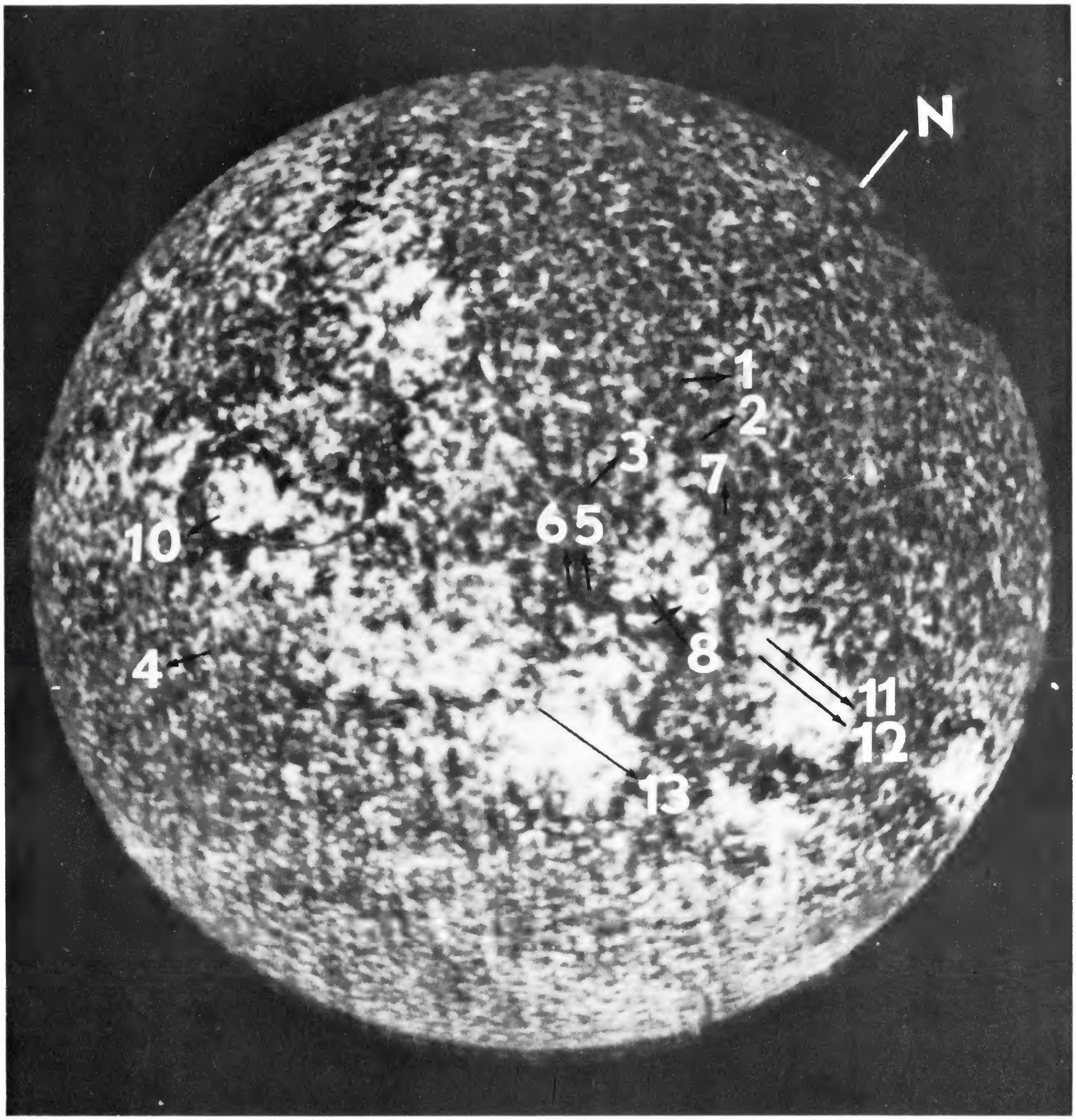

FIG. 1.—An enlargement of one of the Lα spectroheliograms obtained on 1972 July 10. The arrows show the lines of the microdensitometer scans over specific features. The beginning of the tail of the arrow marks the start of the scan, the tip of the arrow the end. Each arrowhead points to a number which labels the scan. N marks the north heliocentric pole.

PRINZ (*see* page 369)